Toxicology Research

PAPER

View Article Online
View Journal | View Issue

Cite this: *Toxicol. Res.*, 2016, **5**, 609

Genome-wide transcriptional analysis of silica nanoparticle-induced toxicity in zebrafish embryos

Hejing Hu,[a,b] Qiuling Li,[a,b] Lizhen Jiang,[a,b] Yang Zou,[a,b] Junchao Duan*[a,b] and Zhiwei Sun*[a,b]

Although silica nanoparticles (SiNPs) have a promising application in biomedical fields, there is still a lack of comprehensive understanding of genome-wide transcriptional analysis. This study aims to clarify the toxic effect and molecular mechanisms of SiNPs in zebrafish embryos based on microarray analysis and bioinformatics analysis. Microarray data analysis demonstrated that SiNP-induced toxicity in zebrafish embryos affected expression of 2515 genes, including 1107 genes that were up-regulated and 1408 genes that were down-regulated. These differentially expressed genes were subjected to bioinformatics analysis for exploring the biological processes triggered by SiNPs in zebrafish embryos. Gene ontology analysis showed that SiNPs caused significant changes in gene expression patterns related to many important functions, including response to stimuli, immune response, cellular processes, and embryonic development. In addition, pathway analysis and Signal-net analysis indicated that the gap junction, vascular smooth muscle contraction, and metabolic pathways, apoptosis, the MAPK signaling pathway, the calcium signaling pathway and the JAK-STAT signaling pathway were the most prominent significant pathways in SiNP-induced toxicity in zebrafish embryos. In addition, the results from qRT-PCR and western blot analysis showed that the IL-6 dependent JAK1/STAT3 signaling pathway was activated by SiNPs in zebrafish embryos. In summary, our data will provide compelling clues for further exploration of SiNP-induced toxicity in zebrafish embryos.

Received 19th October 2015,
Accepted 14th January 2016

DOI: 10.1039/c5tx00383k

www.rsc.org/toxicology

Introduction

Nanotechnology has become a pioneering area in biomedical and biotechnological fields; yet, there are increasing concerns about engineered nanoparticles that have the potential to cause adverse toxic effects *in vivo* or *in vitro*.[1–3] Silica nanoparticles (SiNPs) are one of the most widely-used engineered nanoparticles due to their large surface area, fantastic modifiability, and good biocompatibility.[4] In addition, SiNPs are designed as drug delivery carriers in biomedical fields through intravenous administration.[5] Recently, "C-dots", a cancer-targeted diagnostic probe composed of SiNPs that has been approved by the Food and Drug Administration (FDA), have been used in human clinical trials, Stage I.[6] Therefore, it is raising questions about the biological effects and toxicity of SiNPs on human beings. Although several studies including our previous research had already evaluated the cytotoxicity,[7–9] acute toxicity[10] and sub-chronic toxicity[11] of SiNPs, little information is focused on the gene expression profiles of SiNP-induced toxicity.

The zebrafish, as a well-characterized genome "canonical vertebrate" model, has been proposed for the study of genetics as well as human disease.[12] Their rapid reproduction, optical clarity, ease of maintenance, and chemical sensitivity make zebrafish embryos a favorable tool in developmental biology, genetics and toxicology.[13] In addition, the zebrafish is also a correlative and predictive model for assessing biomaterial nanotoxicity.[14] Genome-wide transcriptional analysis is widely-used in large scale quantitative studies for exploring the mechanisms of disease, predicting the function of new chemicals and grouping genes into signaling pathways.[15] However, the transcriptional analysis of nanoparticle-induced toxicity in zebrafish embryos has been limited. So far, only a few studies focused on this issue to evaluate the gene expression of titanium dioxide nanoparticles, hydroxylated fullerenes or nanoparticulate silver.[16,17] As far as we know, there has been no comprehensive genome-wide transcriptional analysis of SiNP-induced toxicity in zebrafish embryos.

Our previous studies had reported that SiNPs caused embryonic toxicity and cardiovascular toxicity in early developing zebrafish embryos, leading to persistent toxic effects on zebrafish larval behavior.[18,19] In this study, we performed

[a]*Department of Toxicology and Sanitary Chemistry, School of Public Health, Capital Medical University, Beijing 100069, P.R. China*
[b]*Beijing Key Laboratory of Environmental Toxicology, Capital Medical University, Beijing 100069, P.R. China. E-mail: jcduan@ccmu.edu.cn, zwsun@ccmu.edu.cn; Fax: +86 010 83911507; Tel: +86 010 83911868, +86 010 83911507*

genome-wide transcriptional analysis to have a total understanding of SiNPs-triggered toxicity *in vivo* with the zebrafish model. A series of microarray analysis and bioinformatics analysis was conducted, including the differentially expressed genes, gene ontology analysis, significant pathway analysis, and signal transduction pathway networks analysis, followed by qRT-PCR and western blot analysis to verify the microarray data.

Materials and methods

Preparation and characterization of SiNPs

SiNPs were prepared using the Stöber method and characterized as described in our previous studies.[20,21] Briefly, 2.5 mL of tetraethylorthosilicate (TEOS, Sigma, USA) was added to 50 mL of premixed ethanol solution, containing 2 mL of ammonia and 1 mL of water. The reaction mixture was kept stirring (150 rpm) at 40 °C for 12 h. After that, the resulting mixture was centrifuged (12 000 rpm, 15 min) to isolate the particles. After washing with deionized water three times, the SiNPs were dispersed in ultrapure water (50 mL) as a stock medium. Suspensions of SiNPs were dispersed using a sonicator (Bioruptor UDC-200, Belgium) for 5 min prior to experimental tests.

Zebrafish husbandry

Albino strain zebrafish were provided by Hunter Biotechnology, Inc., which is accredited by the International Association for Assessment and Accreditation of Laboratory Animal Care (AAALAC). The accreditation number is 001458. The zebrafish were housed in a circulating aquarium system in an environmentally controlled room (28 °C, 80% humidity). The photoperiod was adjusted to a 14 h light/10 h dark cycle. The larval and adult zebrafish were fed with brine shrimp (hatched from eggs in 10 mL of 2 L salt water) twice a day. For the experiments, fertilized eggs were collected and chosen under a stereomicroscope (Nikon, SMZ645, Japan) at 6 and 24 hpf (hours post-fertilization). All embryos were derived from the same spawn of eggs for statistical comparison between the control and treated groups. We confirm that the Institutional Animal Care and Use Committee (IACUC) of Capital Medical University has approved our study. All experiments were performed in compliance with the relevant laws and institutional guidelines.

Intravenous microinjection

Zebrafish embryos were anesthetized with 0.03% tricaine (Sigma, USA) at 48 hpf. The different concentrations of SiNPs were loaded into borosilicate pulled glass capillary needles with an internal diameter of 15 μm and an outer diameter of 18 μm (World Precision Instruments, Sarasota, USA) using an electrode puller (Narishige, PC-10, Japan). The injections were performed using a Microinjector (Zgenebio, PCO-1500, Taiwan). The SiNPs were injected at the ventral end of the Duct of Cuvier (DC) under a stereomicroscope (Nikon, SMZ645, Japan) and the pulse time was controlled to deliver 10 nL of SiNPs. After intravenous microinjection, the zebrafish embryos were transferred to 6-well microplates (30 embryos in 3 mL solution per well) for a treatment period of 24 h. Zebrafish embryos injected with ultrapure water served as a control group.

Microarray analysis

For Affymetrix® microarray profiling, the total RNA was isolated from 30 zebrafish embryos per treatment group using TRIzol reagent (Invitrogen, Carlsbad, Canada) and purified with an RNeasy Mini Kit (Qiagen, Hilden, Germany) according to the manufacturer's protocol. The amount and quality of RNA were determined using a UV-Vis Spectrophotometer (Thermo, NanoDrop 2000, USA) at an absorbance of 260 nm. The mRNA expression profiling was measured using Zebrafish Gene 1.0 ST Array (Affymetrix GeneChip®, USA), which contains 59 302 gene-level probe sets. The microarray analysis was performed using Affymetrix® Expression Console Software (version 1.2.1). Raw data (CEL files) were normalized at the transcript level using the robust multi-array average method (RMA workflow). The median summarization of transcript expressions was calculated. The gene-level data were then filtered to include only those probe sets that are in the 'core' metaprobe list, which represents RefSeq genes.

Bioinformatics analysis

For the microarray data analysis, differentially expressed genes were identified based on the random variance model (RVM) *t*-test. And the differentially expressed genes were considered to be up- or down-regulated with at least $p < 0.05$. Genes with similar expression patterns often facilitate the overlapping functions. Accordingly, the cluster analysis of gene expression patterns was analyzed using Cluster and Java Treeview software.

Gene Ontology (GO) analysis was applied to analyze the main function of the differentially expressed genes according to the GO which is the key functional classification of the National Center for Biotechnology Information (NCBI), which can organize genes into hierarchical categories and uncover the gene regulatory network on the basis of biological processes and molecular function. Specifically, a two-sided Fisher's exact test and chi-square test were used to classify the GO category, and the false discovery rate (FDR) was calculated to correct the *P*-value; the smaller the FDR, the small the error in judging the *P*-value.

Pathway analysis was used to find out the significant pathways of the differential genes according to the Kyoto Encyclopedia of Genes and Genomes (KEGG), Biocarta and Reatome databases. Fisher's exact test was performed to select the significant pathway, and the threshold of significance was considered as $p < 0.05$.

Gene signal transduction networks (Signal-net), based on the KEGG database about the interactions between different gene products and the theory of network biology, are established to illustrate the inter-gene signaling between differentially expressed genes. Networks are stored and presented as

graphs, where nodes are mainly genes and edges represent relation types between the nodes, such as activation or phosphorylation. The degree is defined as the link number of one node with all of the other nodes. Genes with higher degrees occupy more important positions within the network. In addition, the properties of genes are described by Betweenness Centrality (BC) measures, reflecting the intermediary capacity of a node to modulate other interactions between nodes. Finally, the purpose of the signal transduction network analysis was to locate core key regulatory genes that had a stronger capacity to modulate adjacent genes.

Quantitative RT-PCR analysis. Total RNA was extracted from 50 zebrafish embryos per group using TRIzol reagent (Invitrogen, Carlsbad, Canada) according to the manufacturer's protocol. Tissue incorporating all new tissue as well as one or two bone rays proximal to the original cut site was extracted. Equal amounts of total RNA from each sample were reverse transcribed using Thermoscript reverse transcriptase (Invitrogen) using oligo (dT) and random hexamer primers. The qRT-PCR reaction was monitored using the ABI PRISM 7500 Sequence DetectionSystem (Applied Biosystems, CA, USA) and was run with three biological repeats and three duplicated repeats. All levels were normalized to β-actin (18S levels were similar) and fold induction was calculated by setting control conditions to 1. The primers are listed in Table 6.

Western blot analysis. The total protein of SiNPs-treated zebrafish was extracted with the Tissue Protein Rapid Extraction Kit (Keygen, China), and determined by performing the bicinchoninic acid (BCA) protein assay (Pierce, USA). Equal amounts of 100 μg of lysate proteins were loaded into SDS-polyacrylamide gels (12%) and electrophoretically transferred to PVDF membranes (Millipore, USA). After blocking with 5% nonfat milk in TBST for 1 h at room temperature, the membrane was incubated with interleukin 6 (IL-6), Janus family of tyrosine kinase 1 (JAK1), JAK2, Signal Transducer and Activator of Transcription 3 (STAT3), and Suppressor of Cytokine Signaling 1 (SOCS1) (CST, USA) (1 : 1000, rabbit antibodies) overnight at 4 °C. After washing several times with TBST, the membrane was incubated with anti-rabbit IgG secondary antibody (CST, USA) for 1 h at room temperature. Then, the membrane was washed three times with TBST and the antibody-bound proteins were detected using ECL chemiluminescence reagent (Pierce, USA).

Statistical analysis. All statistical analysis was performed using SPSS 16.0 software (SPSS, Chicago, IL, USA). Student's *t*-test was performed for comparisons between two treatment groups. Three or more treatment groups were compared by one-way analysis of variance (ANOVA) followed by the least significant difference (LSD) test. Significant differences were considered at $p < 0.05$.

Results

Characterization of SiNPs

The full characterization of SiNPs was presented in our previous studies.[20,21] The size distribution showed that the average diameter of the SiNPs was approximately 62.14 ± 7.16 nm. The hydrodynamic sizes and Zeta potentials of SiNPs in ultrapure water were approximately 106.8 nm and −38 mV, respectively. In addition, the purity of the SiNPs was higher than 99.9% and no endotoxin was detected in the SiNPs suspensions. Taken together, these results demonstrated that the SiNPs possessed favorable stability and monodispersity in microinjection medium.

Differential gene expression induced by SiNPs

To investigate the possible gene expression change in SiNP-induced toxicity in zebrafish embryos, we performed a genome-wide transcriptional analysis using the Affymetrix GeneChip® (Zebrafish Gene 1.0 ST Array) which contains 59 302 gene-level probe sets. The results showed that compared with the control group, 2515 significant differentially expressed genes were changed triggered by SiNPs, including 1107 genes that were up-regulated and 1408 genes that were down-regulated. The top 20 differentially expressed up-regulated or down-regulated genes between SiNPs and control groups are listed in Tables 1 and 2, respectively. The microarray data discussed in this article have been deposited in the NCBI Gene Expression Omnibus (GEO) and are accessible through (GEO) Series accession number GSE73427.

GO analysis of differential gene expression induced by SiNPs

GO analysis was applied to find the main gene functions that are affected by SiNPs. An interaction network of significant GO terms was assembled into a GO map to describe the prominent functional categories. As shown in Fig. 1, the top 20 up-regulated GOs induced by SiNPs are translation, response to bacteria, response to oxidative stress, the MyD88-dependent toll-like receptor signaling pathway, innate immune response,

Table 1 The top 20 differentially expressed up-regulated genes between SiNPs and control groups in zebrafish embryos

Gene symbol	Geom mean of intensities (SiNPs)	Geom mean of intensities (control)	Fold-change	*P*-Value
cbx7a	77.16	14.16	5.45	8.00×10^{-7}
fosl1a	119.93	30.43	3.94	6.24×10^{-5}
cfb	203.76	63.16	3.23	4.30×10^{-6}
timp2b	231.35	72.67	3.18	5.70×10^{-6}
il1b	50.39	15.92	3.17	0.0051238
si:dkey-8k3.2	66.5	21.15	3.14	1.31×10^{-4}
LOC100329262	228.04	75.08	3.04	$<1 \times 10^{-7}$
socs3b	280.8	96.09	2.92	1.00×10^{-7}
hsp70	70.41	25.06	2.81	0.0404164
si:ch211-122l24.4	46.31	17.69	2.62	2.00×10^{-7}
C6	16.81	6.51	2.58	7.40×10^{-4}
mmp9	27.84	10.95	2.54	4.85×10^{-4}
cxcl-c1c	39.54	16.26	2.43	5.10×10^{-6}
serpine1	37.36	15.92	2.35	0.0011666
junba	34.59	15.16	2.28	5.16×10^{-5}
fos	356.78	156.67	2.28	5.00×10^{-6}
clu	266.98	118.67	2.25	1.50×10^{-6}
LOC100002292	119.65	54.01	2.22	7.00×10^{-7}
cyp24a1	77.05	34.92	2.21	1.11×10^{-5}
socs3a	59.41	26.86	2.21	7.00×10^{-7}

Table 2 The top 20 differentially expressed down-regulated genes between SiNPs and control groups in zebrafish embryos

Gene symbol	Geom mean of intensities (SiNPs)	Geom mean of intensities (control)	Fold-change	*P*-Value
alas2	34.81	85.39	0.41	2.00×10^{-7}
zgc:194626	16.36	36.93	0.44	0.0018908
zgc:112160	11.75	25.65	0.46	0.009318
si:ch211-250g4.3	35.61	75.13	0.47	3.91×10^{-5}
hbbe2	140.42	280.95	0.5	1.58×10^{-5}
LOC100334599	183.2	347.81	0.53	3.26×10^{-5}
LOC100534758	11.52	21.79	0.53	6.90×10^{-4}
gck	12.1	22.8	0.53	0.0031578
epd	53.37	94.81	0.56	4.20×10^{-6}
si:dkey-8e10.3	16.12	28.59	0.56	2.16×10^{-5}
zgc:73075	69.28	124.46	0.56	2.33×10^{-5}
prph2b	51.99	93.14	0.56	2.06×10^{-4}
zgc:92375	8.06	14.17	0.57	1.35×10^{-5}
hbae3	1127.15	1936.55	0.58	6.70×10^{-6}
nt5c2l1	24.96	43.17	0.58	2.23×10^{-4}
si:ch211-125g7.4	16.3	27.89	0.58	0.0011703
grk1b	27.04	46.55	0.58	0.0035199
si:ch211-76l23.4	27.47	46.9	0.59	5.50×10^{-6}
cyp2ad6	13.81	23.48	0.59	1.06×10^{-4}
opn4.1	28.92	48.73	0.59	2.30×10^{-4}

immune response, response to chemical stimuli, negative regulation of peptidase activity, response to viruses, regulation of cell growth, fin regeneration, glomerular basement membrane development, response to starvation, chordate embryonic development, negative regulation of the apoptotic process, the cobalamin metabolic process, the thrombin receptor signaling pathway, translational elongation, epiboly involved in gastrulation with mouth forming second, and muscle organ development. As shown in Fig. 2, the top 20 down-regulated GOs induced by SiNPs are transport, visual perception, ion transport, transmembrane transport, protein-chromophore linkage, phototransduction, the pyrimidine nucleobase catabolic process, signal transduction, the G-protein coupled receptor signaling pathway, oxygen transport, response to stimuli, neurotransmitter transport, the cyclic nucleotide biosynthetic process, potassium ion transport, chloride transport, erythrocyte differentiation, regulation of ion transmembrane transport, biological processes, the tryptophan catabolic process, and calcium ion transmembrane transport.

Pathway analysis of differential gene expression induced by SiNPs

The significant pathways were analyzed according to the functions and interactions of differential genes based on the KEGG database. As shown in Fig. 3, the up-regulation significant pathways are the ribosome, herpes simplex infection, the adipocytokine signaling pathway, salmonella infection, the toll-like receptor signaling pathway, apoptosis, arachidonic acid metabolism, the JAK-STAT signaling pathway, cytokine–cytokine receptor interaction, and the MAPK signaling pathway. Meanwhile, the down-regulation significant pathways induced by SiNPs are involved in the calcium signaling pathway, phototransduction, neuroactive ligand–receptor interaction, purine metabolism, cardiac muscle contraction, gap junction, glycine, serine and threonine metabolism, vascular

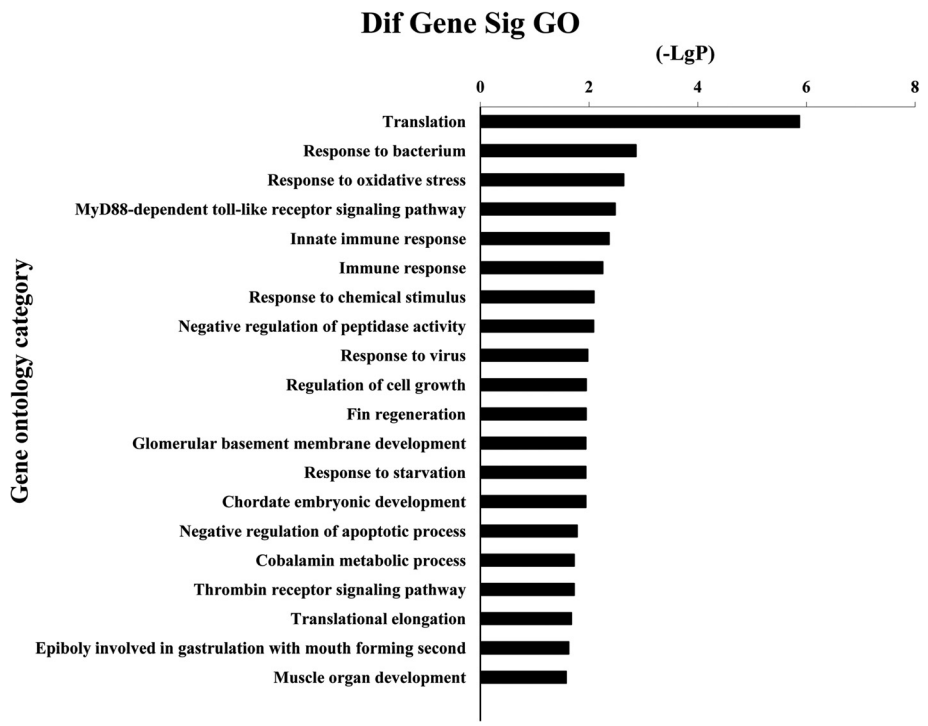

Fig. 1 Significantly changed up-regulation GO of differentially expressed genes induced by SiNPs in zebrafish embryos. The *y* axis shows the GO category and the *x* axis, −lg *P*. The larger −lg *P* indicates a smaller *P*-value.

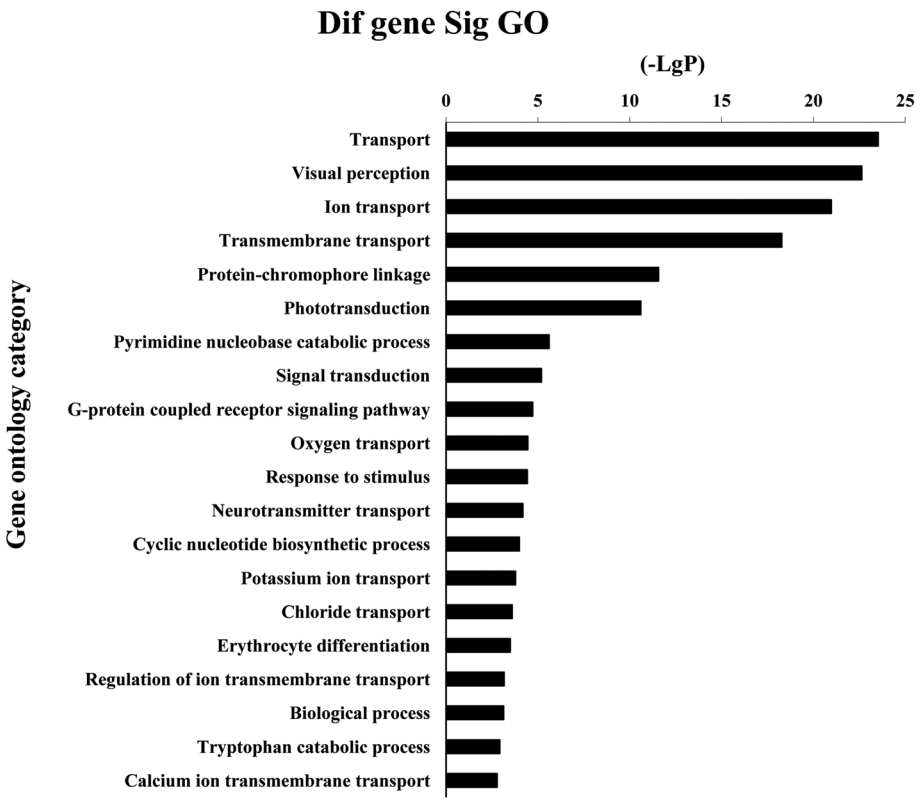

Fig. 2 Significantly changed down-regulation GO of differentially expressed genes induced by SiNPs in zebrafish embryos. The *y* axis shows the GO category and the *x* axis, −lg *P*. The larger −lg *P* indicates a smaller *P*-value.

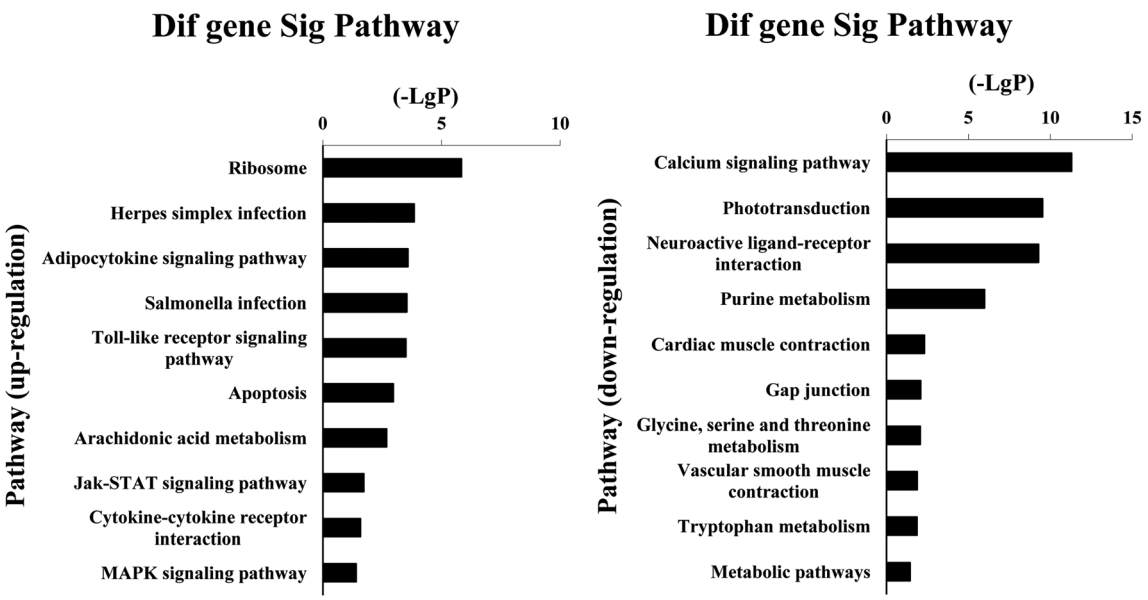

Fig. 3 Significant pathways of differentially expressed up- and down-regulated genes based on the KEGG database. −lg *P*, negative logarithm of the *P* value. *X*-axis denotes that a larger number corresponds to a smaller *P*-value.

smooth muscle contraction, tryptophan metabolism, and metabolic pathways. The summaries of genes that are involved in the up- or down-regulation significant pathways are listed in Tables 3 and 4, respectively.

Signal-net analysis revealed the key genes triggered by SiNPs

Based on the significant GO and pathway analysis, the Signal-net analysis was performed to screen the key genes involved in

Table 3 The summary of 10 up-regulation significant pathways involved in 62 genes

Pathway name	*P*-Value	Gene symbol
Ribosome	1.45106×10^{-6}	rpl30, rpl23, rps12, rps3a, rpl13, rps7, rps27.2, rpl26, rps20, rpl5b, rpl23a, rplp2, rpl9, rps4x, rplp2l
Herpes simplex infection	0.000141971	nfkbiaa, tnfrsf1a, jak1, c3b, socs3b, traf2b, fos, irf9, zgc:110137, stat1b, il1b, c3c, myd88, ticam1
Adipocytokine signaling pathway	0.000259444	acsl4l, socs3b, traf2b, zgc:163064, lepa, stat3, nfkbiaa, tnfrsf1a, nfkbie
Salmonella infection	0.000291533	myd88, pfn2, il1b, tlr5b, flna, tlr4ba, fos, zgc:91909, klc1b, waslb
Toll-like receptor signaling pathway	0.000317561	nfkbiaa, ctsk, tlr5b, myd88, ticam1, tlr4ba, cd40, stat1b, il1b, fos
Apoptosis	0.001081606	il1b, ppp3ccb, si:dkey-260c8.4, myd88, capn2a, prkacbb, nfkbiaa, tnfrsf1a, traf2b
Arachidonic acid metabolism	0.002077218	ptgs2b, ptgs1, ptgs2a, ptges, cpla2, ephx2
Jak-STAT signaling pathway	0.018760723	stat1b, stat3, lepa, jak1, il6st, irf9, socs3b, il13ra1
Cytokine-cytokine receptor interaction	0.026168443	il13ra1, il1b, tnfrsf1a, cxcr4b, lepa, zgc:163064, LOC100333821, cd40, il6st
MAPK signaling pathway	0.039526399	il1b, dusp1, fos, mknk2b, dusp5, flna, si:dkey-260c8.4, hsp70, relb, tnfrsf1a, cpla2, prkacbb, ppp3ccb, traf2b

Table 4 The summary of 10 down-regulation significant pathways involved in 145 genes

Pathway name	*P*-Value	Gene symbol
Calcium signaling pathway	5.00311×10^{-12}	LOC563297, adrb2a, slc25a6, drd1b, slc8a4a, adcy1b, cacna1ab, ryr1b, grin2ab, ptgfr, LOC572143, camk2g1, LOC792634, LOC793708, cacna1da, atp2a1l, grm1a, adcy1a, atp2b2, ptger1a, LOC559964, si:rp71-17i16.4, grin1b, LOC100333648, tnnc1a, htr5al, prkacba, si:dkey-28b4.8, LOC560875, ryr3, LOC560410, si:dkey-206f10.1, chrm5b, plcd3b
Phototransduction	2.95911×10^{-10}	guca1a, rho, arr3a, grk1b, gngt1, pde6a, gnat2, grk7a, rcvrna, cnga1, grk1a, gucy2f, rgs9a
Neuroactive ligand-receptor interaction	5.27801×10^{-10}	grik4, thrab, grm1a, npffr2.1, chrm5b, ptger1a, gabra6b, chrna3, grm6a, grin2ab, zgc:194845, gabrd, ptgfr, LOC100002481, LOC563297, adrb2a, LOC566922, gabrg3, drd1b, LOC100330681, LOC100333578, LOC100333648, gria3a, glra3, adra2b, npy8br, chrnb3b, gria3b, htr5al, prlra, gria4a, agtr2, zgc:110204, gabrg2, grin1b, taar12b, LOC572143, si:dkey-27p18.2, LOC792634, LOC100329592, LOC100330554, chrnb3a
Purine metabolism	1.03734×10^{-6}	si:dkey-206f10.1, nt5e, adcy1b, pde6c, LOC100330875, impdh1a, pde9a, pde6a, ntpcr, gucy2f, nme2a, uox, adcy1a, prhoxnb, LOC560410, pde5ab, LOC100003595, entpd3, entpd2a.1, adss, gucy1b3
Cardiac muscle contraction	0.004858614	cacng7a, atp1b2b, LOC564883, cacna1da, LOC559964, tnnc1a, cacna2d4a, atp1a3b, LOC793708
Gap junction	0.008232007	cx35b, drd1b, prkacba, LOC560410, si:dkey-206f10.1, gucy1b3, LOC100330875, adcy1b, grm1a, adcy1a, LOC792634
Glycine, serine and threonine metabolism	0.008728139	alas2, mao, agxta, zgc:172341, LOC100331665, alas1
Vascular smooth muscle contraction	0.013365257	adcy1a, LOC559964, adcy1b, LOC793708, gucy1b3, kcnma1b, LOC560410, LOC100330875, prkacba, cacna1da, si:dkey-206f10.1
Tryptophan metabolism	0.013820823	cyp1c1, mao, tdo2a, haao, kmo, aanat1
Metabolic pathways	0.036557593	LOC100331665, tdo2a, sgpl1, dpys, gad1a, si:ch73-107c13.2, st6galnac1.1, zgc:172341, si:dkey-91i10.3, glceb, aanat1, galnt13, nme2a, rev3l, atp6ap1a, LOC100003595, plcd3b, ntpcr, pigm, eno1b, rdh8b, hkdc1, ckmt1, atp6v0cb, dgat1a, LOC555478, LOC557518, prhoxnb, kmo, pemt, haao, hmgcs1, sptlc3, pgls, alas1, gck, nt5e, alas2, agxta, uox, aldoca, gal3st1, ext1c, upp1, adss, fbp2, st6galnac6, impdh1a, wu:fj21g01, etnk2, mao, dhrs13l1, pip5k1ca

SiNP-induced toxicity in zebrafish embryos. As shown in Fig. 4, there was a total number of 127 key genes that were obtained in the transduction network. Our results indicated that the genes with high degrees as listed in Table 5 were *entpd3* (ectonucleoside triphosphate diphosphohydrolase 3), *nme2a* (NME/NM23 nucleoside diphosphate kinase 2a), the *adcy* (adenylate cyclase) family, the *pde* (phosphodiesterase) family, *polr2d* (polymerase (RNA) II polypeptide D), *nt5e* (5-nucleotidase, ecto), *ntpcr* (nucleoside-triphosphatase, cancer-related), *entpd2a.1* (ectonucleoside triphosphate diphosphohydrolase 2a.1), the *gucy* family (guanylate cyclase), the *prkac* family (protein kinase, cAMP-dependent, catalytic), *socs3b* (suppressor of cytokine signaling 3b), *rho* (rhodopsin), *cpla2* (cytosolic phospholipase a2), *gna14* (guanine nucleotide binding protein, alpha 14), *hkdc1* (hexokinase domain containing 1), *pip5k1ca* (phosphatidylinositol-4-phosphate 5-kinase, type I, gamma a), *pikfyve* (phosphoinositide kinase, FYVE finger containing), the *jak* family (Janus kinase), *fbp2* (fructose-1,6-bisphosphatase 2), *f2r* (coagulation factor II/thrombin receptor), *itgb4* (integrin, beta 4), the *grk* family (G-protein-coupled receptor kinase).

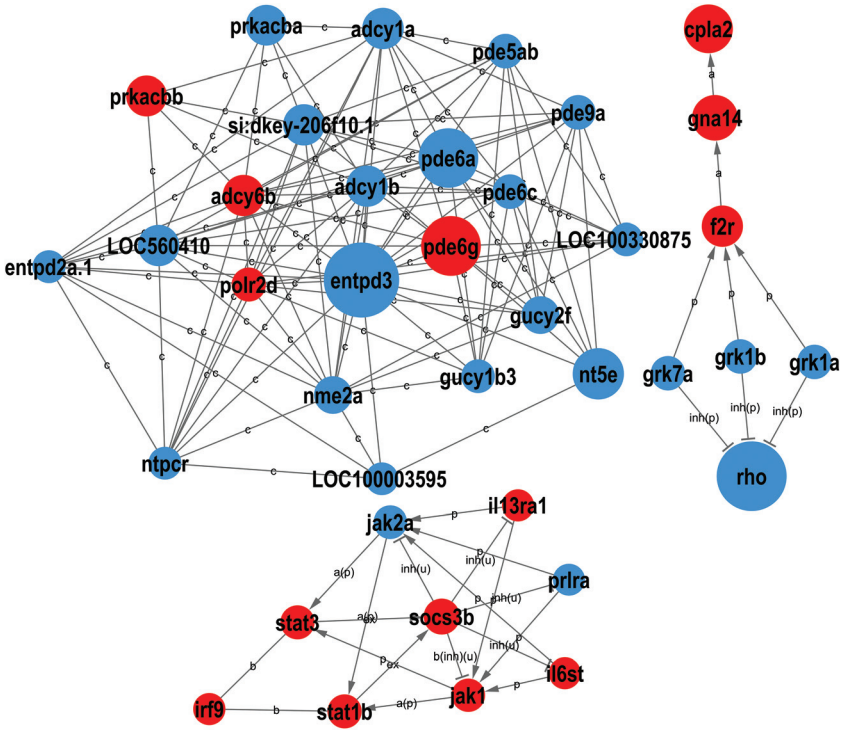

Fig. 4 Signal-net of SiNP-induced toxicity in zebrafish embryos. The red circle represents the up-regulated genes and the blue circles down-regulated genes. The area of the circle represents the degree. Interaction between the genes is shown as: *a* activation, *a(u)* activation (ubiquination), *u* ubiquination, *inh u* inhibition (ubiquination), *b* binding/association, *p* phosphorylation, *inh(–p)* inhibition (dephosphorylation), *a(+p)* activation (phosphorylation), *ind* indirect effect, *inh* inhibition, *disso* dissociation, *ex* expression, *c* compound, *a(ind)* activation (indirect effect), *p(ind)* phosphorylation (indirect effect), *inh(+p)* inhibition (phosphorylation), *m* missing interaction, and *inh(ind)* inhibition (indirect effect).

IL-6 dependent JAK/STAT pathways activated by SiNPs

As shown in Fig. 5A from the qRT-PCR analysis, the gene expressions of il6st, jak1, stat3, and stat1b were significantly increased compared to that of the control, while the expression of jak2a and socs3b was markedly declined. Results from the western blot assay showed that the protein levels of IL-6, JAK1 and STAT3 were gradually up-regulated; whereas the protein expressions of JAK2 and SOCS1 were down-regulated in a dose-dependent manner. Our data demonstrated that the IL-6 dependent JAK1/STAT3 signaling pathway was activated by SiNPs in zebrafish embryos.

Discussion

Although their unique physico-chemical properties make nanoparticles attractive for biomedical applications, nanotoxicity research is gaining attention as nanoparticles unavoidably become part of our daily life. Besides our findings on cardiovascular toxicity induced by SiNPs, other studies also evaluated the uptake, embryonic toxicity, and neurotoxicity in zebrafish models.[22–24] However, as far as we know, there has been no comprehensive genome-wide transcriptional analysis for SiNP-induced toxicity in zebrafish embryos. In this study, we performed the genome-wide transcriptional analysis to have a comprehensive understanding of SiNP-induced toxicity in zebrafish embryos *via* the cluster analysis of gene expression patterns, GO analysis, pathway analysis, and the Signal-net analysis.

GO analysis, recognized as the classical method for the functional annotation of molecular aspects, was used to organize differentially expressed genes into hierarchical categories based on their pertinent biological processes.[25,26] Our study demonstrated that SiNPs could affect the expression of many genes with important functions in zebrafish embryos (Fig. 1 and 2). The subnetworks of the GO analysis could further be clustered into five functions: (1) response to stimuli: response to oxidative stress, starvation, bacteria, viruses and chemicals; (2) immune: innate immune response; (3) cellular processes: transport, biological processes, catabolic processes, peptidase activity, signal transduction, cell growth, and the apoptotic process; (4) embryonic development: chordate embryonic development, erythrocyte differentiation, fin regeneration, glomerular basement membrane development, muscle organ development, and visual perception; (5) cell signaling: the MyD88-dependent toll-like receptor signaling pathway, the thrombin receptor signaling pathway, and the G-protein coupled receptor signaling pathway. It is well known that oxidative stress is the major mechanism for nanoparticle-caused toxicity *in vivo* or *in vitro*.[27–29] The surface chemical structure of SiNPs contains a lot of hydroxyl radicals (˙OH), which have a great tendency to induce oxidative stress and

Table 5 The top genes ranked by degree over 5 after analysis of Signal-Net

Gene symbol	Gene description	Style	Degree	Indegree	Outdegree
entpd3	Ectonucleoside triphosphate diphosphohydrolase 3	Down	22	22	22
nme2a	NME/NM23 nucleoside diphosphate kinase 2a	Down	14	14	14
si:dkey-206f10.1	si:dkey-206f10.1	Down	13	13	12
adcy6b	Adenylate cyclase 6b	Up	13	13	12
adcy1b	Adenylate cyclase 1b	Down	13	13	12
adcy1a	Adenylate cyclase 1a	Down	13	13	12
LOC560410	Adenylate cyclase type 8-like	Down	13	13	12
pde6a	Phosphodiesterase 6A, cGMP-specific, rod, alpha	Down	12	12	10
pde6g	Phosphodiesterase 6G, cGMP-specific, rod, gamma	Up	12	12	10
polr2d	Polymerase (RNA) II (DNA directed) polypeptide D	Up	12	12	12
nt5e	5-Nucleotidase, ecto (CD73)	Down	10	10	10
pde5ab	Phosphodiesterase 5A, cGMP-specific, b	Down	10	10	10
pde9a	Phosphodiesterase 9A	Down	10	10	10
pde6c	Phosphodiesterase 6C, cGMP-specific, cone, alpha prime	Down	10	10	10
ntpcr	Nucleoside-triphosphatase, cancer-related	Down	10	10	10
entpd2a.1	Ectonucleoside triphosphate diphosphohydrolase 2a.1	Down	10	10	10
gucy2f	Guanylate cyclase 2F, retinal	Down	9	9	8
prkacbb	Protein kinase, cAMP-dependent, catalytic, beta b	Up	8	5	8
prkacba	Protein kinase, cAMP-dependent, catalytic, beta a	Down	8	5	8
si:ch211-234p18.3	si:ch211-234p18.3	Down	8	8	8
gucy1b3	Guanylate cyclase 1, soluble, beta 3	Down	8	8	8
LOC100330875	Guanylate cyclase soluble subunit alpha-2-like	Down	8	8	8
socs3b	Suppressor of cytokine signaling 3b	Up	7	2	5
rho	Rhodopsin	Down	6	4	2
cpla2	Cytosolic phospholipase a2	Up	6	6	5
gna14	Guanine nucleotide binding protein (G-protein), alpha 14	Up	6	5	1
hkdc1	Hexokinase domain containing 1	Down	6	6	6
pip5k1ca	Phosphatidylinositol-4-phosphate 5-kinase, type I, gamma	Down	6	3	6
pikfyve	Phosphoinositide kinase, FYVE finger containing	Down	6	3	6
jak2a	Janus kinase 2a	Down	6	4	2
jak1	Janus kinase 1	Up	6	4	2
fbp2	Fructose-1,6-bisphosphatase 2	Down	5	5	5
f2r	Coagulation factor II (thrombin) receptor	Up	5	4	2
itgb4	Integrin, beta 4	Up	5	5	2
grk7a	G-protein-coupled receptor kinase 7a	Down	5	1	4
grk1a	G-protein-coupled receptor kinase 1a	Down	5	1	4
grk1b	G-protein-coupled receptor kinase 1b	Down	5	1	4
LOC100003595	Novel protein similar to vertebrate adenylate cyclase family	Down	5	5	5

Table 6 Primers used for quantitative real-time PCR

Gene name	Forward	Reverse
il6st	GAGAATCATCCCGGCGAGAG	GCATCATCCACAACGGGAGA
jak1	GCAGGCAACTGTGTGTGAAG	AGAACTCGAGCTGGTGTGTG
jak2a	AATCCACTGAATGCGGGGTT	AATTACCCTTCCCCAGCAGC
stat3	GCTTCAGCAGAAGGTCTCGT	GATGACAAGGGGTCGGTCAG
stat1b	GCCACCGGTTAAATGGGAAC	GTGCCTGGAGCTTTGTCTCT
socs3b	ATAGTAGGCTTGACAGCGCC	GAAGCCACTCTCCTGCAGTT
actin	GATGCGGAAACTGGCAAAGG	GAGGGCAAAGTGGTAAACGC

cause extensive damage in cells.[30] Moreover, SiNPs could also induce the endoplasmatic reticulum (ER) stress response in cells.[31] Prolonged and enduring ER stress is thought to be essential to the pathogenesis of inflammatory diseases.[32] In zebrafish, neutrophils and macrophages are the two major cell types involved in the innate immune response.[33] The SiNP-induced oxidative stress and immune response could lead to adverse effects on cellular processes, cell signaling and embryonic development.

Based on the KEGG database, the significance level of pathways of the SiNP-induced differentially expressed genes in zebrafish embryos was detected by pathway analysis.[34] Our data showed that among the significant up-regulation pathways, the toll-like receptor signaling pathway, apoptosis, and the MAPK signaling pathway were well reported in nanoparticle-induced toxicity: nanoparticles could induce immune cell phagocytic activity,[35] inflammation,[36] DNA damage,[37] and immune responses[38] *via* the toll-like receptor signaling

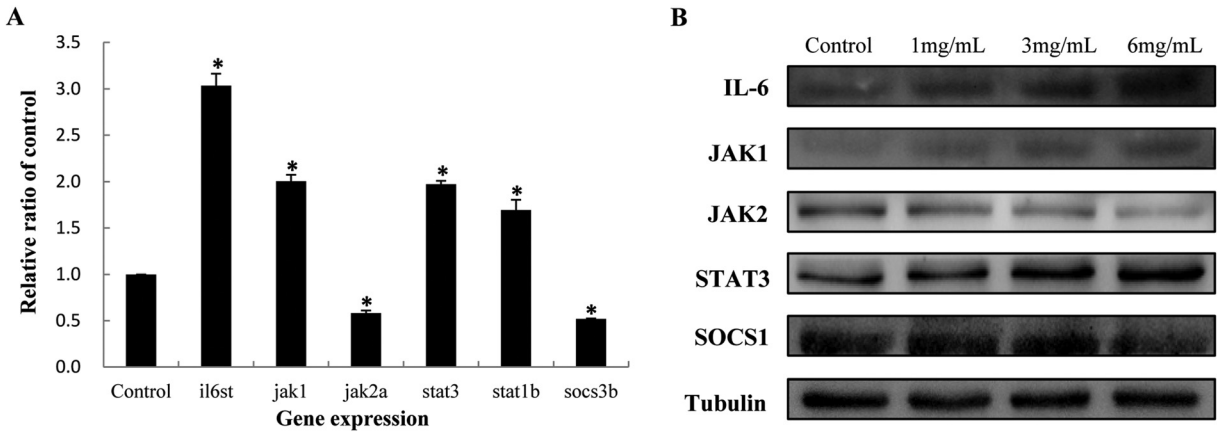

Fig. 5 Effect of SiNPs on the JAK/STAT signaling pathway in zebrafish embryos. (A) qRT-PCR analysis showed that the gene expressions of *il6st, jak1, stat3,* and *stat1b* were significantly increased while those of *jak2a* and *socs3b* were markedly declined. (B) Western blot assay showed that the protein levels of IL-6, JAK1 and STAT3 were gradually up-regulated; whereas the protein expressions of JAK2 and SOCS1 were down-regulated. Data are expressed as means ± S.D. from three independent experiments (*$p < 0.05$).

pathway; it has been well-documented that the nanoparticles could trigger the apoptosis pathway;[39–41] cytokine activation, inflammation, oxidative DNA damage, cell cycle arrest, apoptosis, and differentiation of mesenchymal stem cells were induced by nanoparticles *via* the MAPK signaling pathway.[42–44] Meanwhile, the significant down-regulation pathways, the calcium signaling pathway,[45] neuroactive ligand–receptor interaction,[46] gap junction,[47] vascular smooth muscle contraction,[48] and metabolic pathways[49] have been well-documented in nanoparticle-induced toxicity. Further study is needed to explore the rest of the significant pathways induced by SiNPs in zebrafish embryos.

Finally, the Signal-net analysis was performed to have an insight into the inter-gene signaling between the differentially expressed genes. According to the KEGG database and based on the GO analysis and pathway analysis, 127 key genes were collected and a diagram of the gene transduction network is presented in Fig. 4. Among the genes with high degrees as listed in Table 5, adcy1a, adcy1b, gucy1b3, and prkacba were involved in gap junction and vascular smooth muscle contraction pathways; nt5e, ntpcr, hkdc1, pip5k1ca, and fbp2 were involved in metabolic pathways; prkacbb and cpla2 were involved in apoptosis and the MAPK signaling pathway; prkacba was involved in the calcium signaling pathway; socs3b and jak1 were involved in the JAK-STAT signaling pathway. Based on the data above, results from the Signal-net analysis indicated that the gap junction, vascular smooth muscle contraction, and metabolic pathways, apoptosis, the MAPK signaling pathway, the calcium signaling pathway and the JAK/STAT signaling pathway were the most prominent significant pathways in SiNP-induced toxicity in zebrafish embryos. However, there was limited information about the nanoparticle-induced toxicity *via* the JAK/STAT signaling pathway. Therefore, we further verified the JAK/STAT signaling pathway using qRT-PCR and western blot analysis. Our data confirmed that the IL-6 dependent JAK1/STAT3 signaling pathway was activated by SiNPs in zebrafish embryos (Fig. 5). The IL-6 mediated JAK/STAT signaling pathway is involved in mechanisms in inflammation and angiogenesis regulation, and mediates endothelial cell growth, survival and apoptosis.[50]

Conclusions

In summary, our study demonstrated that the intravenous microinjection of SiNPs in zebrafish embryos caused significant changes in gene expression patterns. The differentially expressed genes were clustered into hierarchical categories related to response to stimuli, immune response, cellular processes, and embryonic development, which involved several significant pathways, including the gap junction, vascular smooth muscle contraction, and metabolic pathways, apoptosis, the MAPK signaling pathway, the calcium signaling pathway and the JAK-STAT signaling pathway. The verification experiments revealed that the IL-6 dependent JAK1/STAT3 signaling pathway was activated by SiNPs in zebrafish embryos. Our data will provide a comprehensive understanding of genome-wide transcriptional analysis of SiNP-induced toxicity in zebrafish embryos. Further study is required to verify the underlying mechanisms involved in this issue.

Conflict of interest

The authors declare they have no conflict of interest.

Acknowledgements

This work was supported by the National Natural Science Foundation of China (no. 81502830, 81230065), the Training

Programme Foundation for the Talents by the Beijing Ministry of Education (2014000020124G152), and the Special Project of Beijing Municipal Science & Technology Commission (KZ201410025022). The authors thank Prof. Wensheng Yang from Jilin University for the preparation of the SiNPs, Weiping Tang of Cnkingbio biotechnology Co. Ltd for bioinformatics assistance, and Hongcui Liu of Hunter Biotechnology, Inc. for technical support.

References

1 Y. M. Long, X. C. Zhao, A. C. Clermont, Q. F. Zhou, Q. Liu, E. P. Feener, B. Yan and G. B. Jiang, Negatively charged silver nanoparticles cause retinal vascular permeability by activating plasma contact system and disrupting adherens junction, *Nanotoxicology*, 2015, 1–11.

2 H. Arami, A. Khandhar, D. Liggitt and K. M. Krishnan, In vivo delivery, pharmacokinetics, biodistribution and toxicity of iron oxide nanoparticles, *Chem. Soc. Rev.*, 2015, **44**, 8576–8607.

3 M. Azhdarzadeh, A. A. Saei, S. Sharifi, M. J. Hajipour, A. M. Alkilany, M. Sharifzadeh, F. Ramazani, S. Laurent, A. Mashaghi and M. Mahmoudi, Nanotoxicology: Advances and pitfalls in research methodology, *Nanomedicine*, 2015, **10**, 2931–2952.

4 N. J. Halas, Nanoscience under glass: The versatile chemistry of silica nanostructures, *ACS Nano*, 2008, **2**, 179–183.

5 Z. Li, J. C. Barnes, A. Bosoy, J. F. Stoddart and J. I. Zink, Mesoporous silica nanoparticles in biomedical applications, *Chem. Soc. Rev.*, 2012, **41**, 2590–2605.

6 M. Benezra, O. Penate-Medina, P. B. Zanzonico, D. Schaer, H. Ow, A. Burns, E. DeStanchina, V. Longo, E. Herz, S. Iyer, J. Wolchok, S. M. Larson, U. Wiesner and M. S. Bradbury, Multimodal silica nanoparticles are effective cancer-targeted probes in a model of human melanoma, *J. Clin. Invest.*, 2011, **121**, 2768–2780.

7 Y. Yu, J. Duan, Y. Yu, Y. Li, X. Liu, X. Zhou, K. F. Ho, L. Tian and Z. Sun, Silica nanoparticles induce autophagy and autophagic cell death in hepg2 cells triggered by reactive oxygen species, *J. Hazard. Mater.*, 2014, **270**, 176–186.

8 J. Duan, Y. Yu, Y. Yu, Y. Li, J. Wang, W. Geng, L. Jiang, Q. Li, X. Zhou and Z. Sun, Silica nanoparticles induce autophagy and endothelial dysfunction via the pi3k/akt/mtor signaling pathway, *Int. J. Nanomed.*, 2014, **9**, 5131–5141.

9 J. Duan, Y. Yu, Y. Li, Y. Yu, Y. Li, X. Zhou, P. Huang and Z. Sun, Toxic effect of silica nanoparticles on endothelial cells through DNA damage response via chk1-dependent g2/m checkpoint, *PLoS One*, 2013, **8**, e62087.

10 Y. Yu, Y. Li, W. Wang, M. Jin, Z. Du, Y. Li, J. Duan, Y. Yu and Z. Sun, Acute toxicity of amorphous silica nanoparticles in intravenously exposed icr mice, *PLoS One*, 2013, **8**, e61346.

11 Z. Du, D. Zhao, L. Jing, G. Cui, M. Jin, Y. Li, X. Liu, Y. Liu, H. Du, C. Guo, X. Zhou and Z. Sun, Cardiovascular toxicity of different sizes amorphous silica nanoparticles in rats after intratracheal instillation, *Cardiovasc. Toxicol.*, 2013, **13**, 194–207.

12 C. E. Hicken, T. L. Linbo, D. H. Baldwin, M. L. Willis, M. S. Myers, L. Holland, M. Larsen, M. S. Stekoll, S. D. Rice, T. K. Collier, N. L. Scholz and J. P. Incardona, Sublethal exposure to crude oil during embryonic development alters cardiac morphology and reduces aerobic capacity in adult fish, *Proc. Natl. Acad. Sci. U. S. A.*, 2011, **108**, 7086–7090.

13 H. Chen, J. Hu, J. Yang, Y. Wang, H. Xu, Q. Jiang, Y. Gong, Y. Gu and H. Song, Generation of a fluorescent transgenic zebrafish for detection of environmental estrogens, *Aquat. Toxicol.*, 2010, **96**, 53–61.

14 V. E. Fako and D. Y. Furgeson, Zebrafish as a correlative and predictive model for assessing biomaterial nanotoxicity, *Adv. Drug Delivery Rev.*, 2009, **61**, 478–486.

15 R. B. Stoughton, Applications of DNA microarrays in biology, *Annu. Rev. Biochem.*, 2005, **74**, 53–82.

16 B. Jovanovic, T. Ji and D. Palic, Gene expression of zebrafish embryos exposed to titanium dioxide nanoparticles and hydroxylated fullerenes, *Ecotoxicol. Environ. Saf.*, 2011, **74**, 1518–1525.

17 R. J. Griffitt, C. M. Lavelle, A. S. Kane, N. D. Denslow and D. S. Barber, Chronic nanoparticulate silver exposure results in tissue accumulation and transcriptomic changes in zebrafish, *Aquat. Toxicol.*, 2013, **130–131**, 192–200.

18 J. Duan, Y. Yu, Y. Li, Y. Yu and Z. Sun, Cardiovascular toxicity evaluation of silica nanoparticles in endothelial cells and zebrafish model, *Biomaterials*, 2013, **34**, 5853–5862.

19 J. Duan, Y. Yu, H. Shi, L. Tian, C. Guo, P. Huang, X. Zhou, S. Peng and Z. Sun, Toxic effects of silica nanoparticles on zebrafish embryos and larvae, *PLoS One*, 2013, **8**, e74606.

20 J. Duan, Y. Yu, Y. Yu, Y. Li, P. Huang, X. Zhou, S. Peng and Z. Sun, Silica nanoparticles enhance autophagic activity, disturb endothelial cell homeostasis and impair angiogenesis, *Part. Fibre Toxicol.*, 2014, **11**, 50.

21 J. Duan, Y. Yu, Y. Li, Y. Li, H. Liu, L. Jing, M. Yang, J. Wang, C. Li and Z. Sun, Low-dose exposure of silica nanoparticles induces cardiac dysfunction via neutrophil-mediated inflammation and cardiac contraction in zebrafish embryos, *Nanotoxicology*, 2015, 1–11, DOI: 10.3109/17435390.2015.1102981, [Epub ahead of print].

22 X. Li, B. Liu, X. L. Li, Y. X. Li, M. Z. Sun, D. Y. Chen, X. Zhao and X. Z. Feng, Sio2 nanoparticles change colour preference and cause parkinson's-like behaviour in zebrafish, *Sci. Rep.*, 2014, **4**, 3810.

23 K. Fent, C. J. Weisbrod, A. Wirth-Heller and U. Pieles, Assessment of uptake and toxicity of fluorescent silica nanoparticles in zebrafish (danio rerio) early life stages, *Aquat. Toxicol.*, 2010, **100**, 218–228.

24 T. P. Liu, S. H. Wu, Y. P. Chen, C. M. Chou and C. T. Chen, Biosafety evaluations of well-dispersed mesoporous silica nanoparticles: Towards in vivo-relevant conditions, *Nanoscale*, 2015, **7**, 6471–6480.

25 C. Lu, M. Xiong, Y. Luo, J. Li, Y. Zhang, Y. Dong, Y. Zhu, T. Niu, Z. Wang and L. Duan, Genome-wide transcriptional

analysis of apoptosis-related genes and pathways regulated by h2ax in lung cancer a549 cells, *Apoptosis*, 2013, **18**, 1039–1047.

26 M. Ashburner, C. A. Ball, J. A. Blake, D. Botstein, H. Butler, J. M. Cherry, A. P. Davis, K. Dolinski, S. S. Dwight, J. T. Eppig, M. A. Harris, D. P. Hill, L. Issel-Tarver, A. Kasarskis, S. Lewis, J. C. Matese, J. E. Richardson, M. Ringwald, G. M. Rubin and G. Sherlock, Gene ontology: Tool for the unification of biology. The gene ontology consortium, *Nat. Genet.*, 2000, **25**, 25–29.

27 M. Khatri, D. Bello, P. Gaines, J. Martin, A. K. Pal, R. Gore and S. Woskie, Nanoparticles from photocopiers induce oxidative stress and upper respiratory tract inflammation in healthy volunteers, *Nanotoxicology*, 2013, **7**, 1014–1027.

28 A. Mendoza, J. A. Torres-Hernandez, J. G. Ault, J. H. Pedersen-Lane, D. Gao and D. A. Lawrence, Silica nanoparticles induce oxidative stress and inflammation of human peripheral blood mononuclear cells, *Cell Stress Chaperones*, 2014, **19**, 777–790.

29 R. Alinovi, M. Goldoni, S. Pinelli, M. Campanini, I. Aliatis, D. Bersani, P. P. Lottici, S. Iavicoli, M. Petyx, P. Mozzoni and A. Mutti, Oxidative and pro-inflammatory effects of cobalt and titanium oxide nanoparticles on aortic and venous endothelial cells, *Toxicol. In Vitro*, 2015, **29**, 426–437.

30 D. Napierska, L. C. Thomassen, D. Lison, J. A. Martens and P. H. Hoet, The nanosilica hazard: Another variable entity, *Part. Fibre Toxicol.*, 2010, **7**, 39.

31 V. Christen and K. Fent, Silica nanoparticles and silver-doped silica nanoparticles induce endoplasmatic reticulum stress response and alter cytochrome P4501A activity, *Chemosphere*, 2012, **87**, 423–434.

32 G. Liu, N. Liu, Y. Xu, Y. Ti, J. Chen, J. Chen, J. Zhang and J. Zhao, Endoplasmic reticulum stress-mediated inflammatory signaling pathways within the osteolytic periosteum and interface membrane in particle-induced osteolysis, *Cell Tissue Res.*, 2015, DOI: 10.1007/s00441-015-2205-9.

33 J. R. Mathias, M. E. Dodd, K. B. Walters, S. K. Yoo, E. A. Ranheim and A. Huttenlocher, Characterization of zebrafish larval inflammatory macrophages, *Dev. Comp. Immunol.*, 2009, **33**, 1212–1217.

34 M. Yi, J. D. Horton, J. C. Cohen, H. H. Hobbs and R. M. Stephens, Wholepathwayscope: A comprehensive pathway-based analysis tool for high-throughput data, *BMC Bioinf.*, 2006, **7**, 30.

35 A. Pinsino, R. Russo, R. Bonaventura, A. Brunelli, A. Marcomini and V. Matranga, Titanium dioxide nanoparticles stimulate sea urchin immune cell phagocytic activity involving tlr/p38 mapk-mediated signalling pathway, *Sci. Rep.*, 2015, **5**, 14492.

36 H. Babazada, F. Yamashita, S. Yanamoto and M. Hashida, Self-assembling lipid modified glycol-split heparin nanoparticles suppress lipopolysaccharide-induced inflammation through tlr4-nf-kappab signaling, *J. Controlled Release*, 2014, **194**, 332–340.

37 K. S. El-Said, E. M. Ali, K. Kanehira and A. Taniguchi, Molecular mechanism of DNA damage induced by titanium dioxide nanoparticles in toll-like receptor 3 or 4 expressing human hepatocarcinoma cell lines, *J. Nanobiotechnol.*, 2014, **12**, 48.

38 J. M. Silva, E. Zupancic, G. Vandermeulen, V. G. Oliveira, A. Salgado, M. Videira, M. Gaspar, L. Graca, V. Preat and H. F. Florindo, In vivo delivery of peptides and toll-like receptor ligands by mannose-functionalized polymeric nanoparticles induces prophylactic and therapeutic anti-tumor immune responses in a melanoma model, *J. Controlled Release*, 2015, **198**, 91–103.

39 M. Morales-Cruz, C. M. Figueroa, T. Gonzalez-Robles, Y. Delgado, A. Molina, J. Mendez, M. Morales and K. Griebenow, Activation of caspase-dependent apoptosis by intracellular delivery of cytochrome c-based nanoparticles, *J. Nanobiotechnol.*, 2014, **12**, 33.

40 Y. H. Lee, F. Y. Cheng, H. W. Chiu, J. C. Tsai, C. Y. Fang, C. W. Chen and Y. J. Wang, Cytotoxicity, oxidative stress, apoptosis and the autophagic effects of silver nanoparticles in mouse embryonic fibroblasts, *Biomaterials.*, 2014, **35**, 4706–4715.

41 V. Sharma, D. Anderson and A. Dhawan, Zinc oxide nanoparticles induce oxidative DNA damage and ros-triggered mitochondria mediated apoptosis in human liver cells (hepg2), *Apoptosis*, 2012, **17**, 852–870.

42 D. Couto, M. Freitas, G. Porto, M. A. Lopez-Quintela, J. Rivas, P. Freitas, F. Carvalho and E. Fernandes, Polyacrylic acid-coated and non-coated iron oxide nanoparticles induce cytokine activation in human blood cells through tak1, p38 mapk and jnk pro-inflammatory pathways, *Arch. Toxicol.*, 2015, **89**, 1759–1769.

43 H. J. Eom and J. Choi, P38 mapk activation, DNA damage, cell cycle arrest and apoptosis as mechanisms of toxicity of silver nanoparticles in jurkat t cells, *Environ. Sci. Technol.*, 2010, **44**, 8337–8342.

44 C. Yi, D. Liu, C. C. Fong, J. Zhang and M. Yang, Gold nanoparticles promote osteogenic differentiation of mesenchymal stem cells through p38 mapk pathway, *ACS Nano*, 2010, **4**, 6439–6448.

45 L. Mores, E. L. Franca, N. A. Silva, E. A. Suchara and A. C. Honorio-Franca, Nanoparticles of barium induce apoptosis in human phagocytes, *Int. J. Nanomed.*, 2015, **10**, 6021–6026.

46 T. Borisova, A. Nazarova, M. Dekaliuk, N. Krisanova, N. Pozdnyakova, A. Borysov, R. Sivko and A. P. Demchenko, Neuromodulatory properties of fluorescent carbon dots: Effect on exocytotic release, uptake and ambient level of glutamate and gaba in brain nerve terminals, *Int. J. Biochem. Cell Biol.*, 2015, **59**, 203–215.

47 N. Ale-Agha, C. Albrecht and L. O. Klotz, Loss of gap junctional intercellular communication in rat lung epithelial cells exposed to carbon or silica-based nanoparticles, *Biol. Chem.*, 2010, **391**, 1333–1339.

48 W. C. Chiu, J. M. Juang, S. N. Chang, C. K. Wu, C. T. Tsai, C. D. Tseng, Y. Z. Tseng, M. J. Su and F. T. Chiang, Differ-

ential baseline expression and angiotensin ii-stimulation of leukemia-associated rhogef in vascular smooth muscle cells of spontaneously hypertensive rats, *Int. J. Nanomed.*, 2012, **7**, 5929–5939.

49 V. S. Periasamy, J. Athinarayanan, A. M. Al-Hadi, F. A. Juhaimi and A. A. Alshatwi, Effects of titanium dioxide nanoparticles isolated from confectionery products on the metabolic stress pathway in human lung fibroblast cells, *Arch. Environ. Contam. Toxicol.*, 2015, **68**, 521–533.

50 R. I. Osmond, S. Das and M. F. Crouch, Development of cell-based assays for cytokine receptor signaling, using an alphascreen surefire assay format, *Anal. Biochem.*, 2010, **403**, 94–101.